Genetic lesions associated with chronic lymphocytic leukemia transformation to Richter syndrome

Giulia Fabbri,[1] Hossein Khiabanian,[4] Antony B. Holmes,[1] Jiguang Wang,[4] Monica Messina,[1,5] Charles G. Mulligan,[6] Laura Pasqualucci,[1,2] Raul Rabadan,[4] and Riccardo Dalla-Favera[1,2,3]

[1]Institute for Cancer Genetics, Herbert Irving Comprehensive Cancer Center, [2]Department of Pathology and Cell Biology, [3]Departments of Genetics and Development and of Microbiology and Immunology and [4]Department of Biomedical Informatics and Center for Computational Biology and Bioinformatics, Columbia University, New York, NY 10032
[5]Division of Hematology, Department of Hematology and Cellular Biotechnologies, Sapienza University, 00161 Roma, Italy
[6]Department of Pathology, St. Jude Children's Research Hospital, Memphis, TN 38105

Richter syndrome (RS) derives from the rare transformation of chronic lymphocytic leukemia (CLL) into an aggressive lymphoma, most commonly of the diffuse large B cell lymphoma (DLBCL) type. The molecular pathogenesis of RS is only partially understood. By combining whole-exome sequencing and copy-number analysis of 9 CLL–RS pairs and of an extended panel of 43 RS cases, we show that this aggressive disease typically arises from the predominant CLL clone by acquiring an average of ~20 genetic lesions/case. RS lesions are heterogeneous in terms of load and spectrum among patients, and include those involved in CLL progression and chemorefractoriness (*TP53* disruption and *NOTCH1* activation) as well as some not previously implicated in CLL or RS pathogenesis. In particular, disruption of the *CDKN2A/B* cell cycle regulator is associated with ~30% of RS cases. Finally, we report that the genomic landscape of RS is significantly different from that of de novo DLBCL, suggesting that they represent distinct disease entities. These results provide insights into RS pathogenesis, and identify dysregulated pathways of potential diagnostic and therapeutic relevance.

CORRESPONDENCE
Riccardo Dalla-Favera:
rd10@columbia.edu

Abbreviations used: CLL, chronic lymphocytic leukemia; CNA, copy number abberation; DLBCL, diffuse large B cell lymphoma; FISH, fluorescence in situ hybridization; RS, Richter syndrome; SNP, single-nucleotide polymorphism; WES, whole-exome sequencing.

Richter syndrome (RS) is defined as the development of a lymphoma, most commonly of the diffuse large B cell lymphoma (DLBCL) type, during the clinical progression of B cell chronic lymphocytic leukemia (CLL; Swerdlow, 2008; Rossi and Gaidano, 2009). This event occurs in the natural history of CLL with a cumulative incidence of ~10% (Rossi and Gaidano, 2009). Analysis of immunoglobulin (Ig) gene rearrangements showed that RS derives from the same B cell that originated the CLL clone. Despite being classified histologically as DLBCL, clonally-related RS is characterized by a much poorer outcome, as most of the patients do not respond to standard therapy and succumb rapidly to the disease (Tsimberidou et al., 2008; Rossi et al., 2011b).

The molecular pathogenesis of RS is only partially understood. Inactivation of the *TP53* tumor suppressor gene is observed in ~60% of patients and represents an independent predictor of overall survival after RS transformation (Rossi et al., 2011b). The second most frequent genetic lesions are represented by *NOTCH1* and *MYC* activating events, each occurring in about ~30% of cases (Fabbri et al., 2011; Rossi et al., 2011b). Similar to other examples of evolution of mature B cell–derived tumors from indolent to aggressive disease, *MYC*-activating events often coexist with *TP53* disruption in RS (Yano et al., 1992; Davies et al., 2007), whereas they distribute in a mutually exclusive fashion with *NOTCH1* mutations (Fabbri et al., 2011), consistent with the notion that *NOTCH1* is a direct transcriptional activator of *MYC* expression (Palomero et al., 2006).

G. Fabbri and H. Khiabanian contributed equally to this paper.
R. Rabadan and R. Dalla-Favera contributed equally to this paper.

These genetic abnormalities are often acquired at transformation, suggesting their importance for the establishment and maintenance of the phenotype characteristic of RS (Fabbri et al., 2011; Rossi et al., 2011b).

The known RS-associated genetic lesions have been identified based on candidate gene approaches, do not account for all cases, and most likely represent only a fraction of those associated with RS pathogenesis. Conversely, unbiased, genome-wide methods aimed at the characterization of the entire spectrum of genetic lesions that are acquired by RS can be useful to decipher the clonal evolution pattern occurring in the CLL–RS transition process, to provide further insights into its pathogenesis, and to identify possible differences between RS-associated DLBCL and de novo DLBCL (Morin et al., 2011; Pasqualucci et al., 2011; Lohr et al., 2012; Zhang et al., 2013). Toward this end, we have adopted an integrated approach based on next generation whole-exome sequencing (WES) and genome-wide high-density single-nucleotide polymorphism (SNP) analysis to investigate the RS coding genome.

We report that most RS cases derive from the same clone as CLL cells through a linear evolution pattern involving the acquisition of novel genetic lesions. These lesions are heterogeneous in number and spectrum among RS cases, and include genes not previously associated with RS transformation. Finally, our results demonstrate that RS represents a genetically distinct entity from de novo DLBCL.

RESULTS
Most RS arise through a linear evolution pattern from the CLL predominant clone

Transformation of CLL to RS can occur as a linear process, in which RS is a direct descendant of the initial major CLL clone, or by branched evolution from a common earlier precursor cell that acquired distinct genetic lesions to become a CLL or a RS. To decipher the clonal evolution pattern of CLL to RS, we performed next-generation WES, and copy number (CN) and fluorescence in situ hybridization (FISH) analysis for the detection of translocations known to be recurrent in RS and/or de novo DLBCL (i.e., *MYC*, *BCL6*, and *BCL2* translocations) in a set of nine paired and clonally related CLL-RS cases. In three cases, we also included the specimen corresponding to the terminal leukemic phase of RS (RSII), which represents an extremely rare and aggressive phenotype of the disease, characterized by severe cytopenia and leukemic dissemination of large B cells within the peripheral blood, and invariably associated with patients' death (Table S1; Rossi and Gaidano, 2009). Additionally, an independent set of six paired CLL–RS cases with only CN data available was included in the analysis (total, *n* = 15 pairs).

To reconstruct the evolutionary history of CLL transformation, we assessed separately the load of genetic lesions shared between the two phases of the disease, those present in CLL and absent in RS, and those present in RS but not in CLL (Fig. 1). This analysis allowed us to discriminate between a linear pattern of evolution, in which all CLL lesions are maintained in the RS specimen together with additional RS-specific abnormalities, and a branched pattern of evolution, in which CLL- and RS-specific lesions are present in addition to the set of shared abnormalities. Due to the unavailability of paired normal DNAs, mutations present in both CLL and RS were counted only for genes known to be mutated in CLL (i.e., *NOTCH1*, *SF3B1*, *TP53*, *ATM*, and *MYD88*). Genetic lesions that were only observed in the CLL phase because of CN losses or copy neutral-LOH in RS were not computed in the analysis.

In the majority of RS patients (*n* = 12/15), all the abnormalities identified in the CLL phase of the disease were maintained in the RS phase, which, in turn, acquired a variable number of genetic lesions. This scenario is consistent with a linear pattern of evolution from CLL to RS, as observed for other tumor progression states (Walter et al., 2012; Aparicio and Caldas, 2013) and for a subset of progressed CLLs (Schuh et al., 2012; Landau et al., 2013; Ouillette et al., 2013; Fig. 1; Table S2 and Table S3). In one patient (case 7), a subclonal 13q14 deletion detected by FISH in 9% of the nuclei of CLL cells (Table S1) was not found in the paired RS, suggesting its presence in a minor clone that was not selected for subsequent transformation, and consistent with the notion that absence of del13q14 is associated with a higher risk of transformation (Rossi et al., 2008).

In the remaining three patients (20%), a subset of the lesions identified in the CLL clone was not detectable in the RS specimen. In particular, case 5 harbored one point mutation in the CLL phase that was absent both in the corresponding RS sample and in the final leukemic phase; in case 4, four point mutations were present in CLL at diagnosis and in the terminal leukemic phase, but not in the RS specimen (Fig. 1 and Table S2); in the third patient, characterized only by CN analysis (case 25), ∼35% of CLL lesions (*n* = 8/23) were not maintained in the RS diagnostic sample (Table S3). In all three cases, a variable number of genetic lesions were uniquely present in RS cells. These scenarios are consistent with a branching pattern of evolution, in which a putative precursor carrying the genetic lesions common to CLL and RS has then evolved toward CLL and RS through the acquisition of distinct and independent events.

To address the evolutionary pattern followed in the progression of RS from nodal to leukemic disease, we next focused on the set of lesions present either in the RS or in the RSII phase. Notably, whereas case 2 progressed through a linear evolution pattern, in both case 4 and case 5 the RS and its terminal leukemic phase acquired a totally or partially distinct set of genetic lesions, suggesting their progression through a branching pattern of clonal evolution (Figs. 1–3). In case 4, biallelic *TP53* disruption was acquired in both phases of RS, but this event clearly occurred in different tumor subclones, as documented by the different size of the deletion in 17p and by the distinct *TP53* mutation observed in RS and RSII (R213X and R248Q, respectively; see Fig. 3, a and b). In case 5, multiple genetic lesions ultimately leading to NOTCH signaling activation were acquired during CLL transformation and subsequent RS progression (Fig. 3, c and d). In particular, a *NOTCH1* PEST-truncating mutation (P2514fs) was present in the CLL

2274

Molecular determinants of transformation of CLL to RS | Fabbri et al.
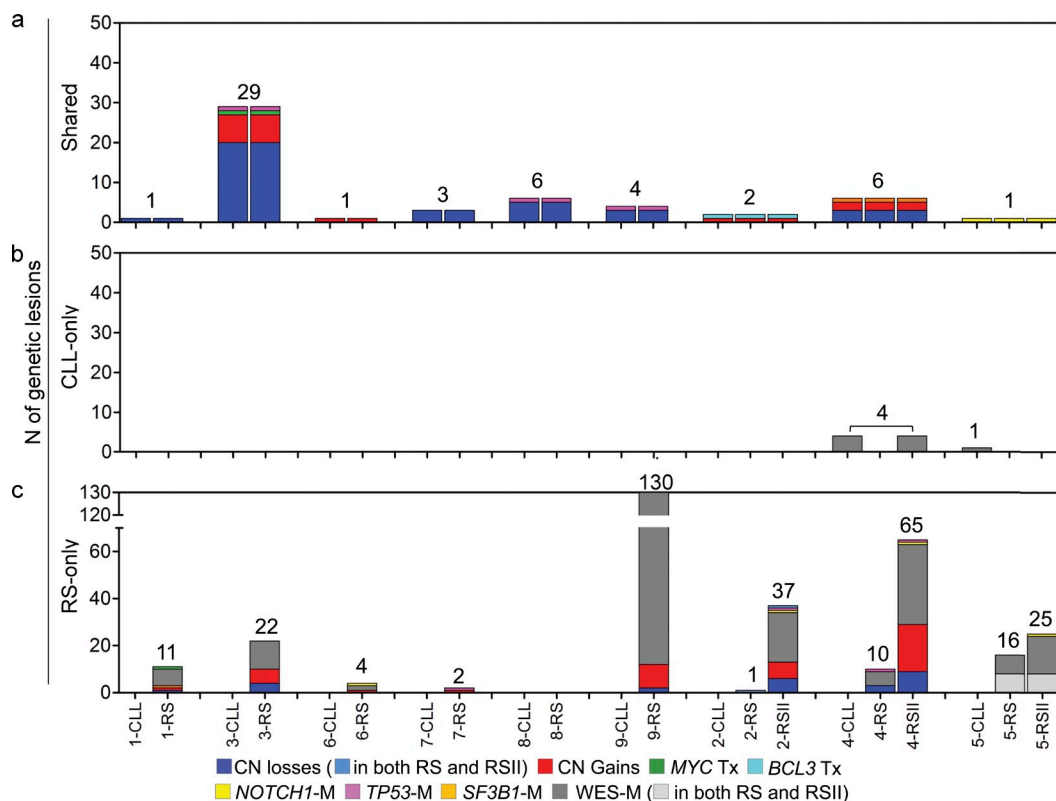
Figure 1. Dynamics of genetic lesions associated with the transformation of CLL to RS. Histograms representing the number of genetic lesions: (a) shared between the 9 CLL and RS discovery pairs (data based on CN and FISH analyses and sequencing of *NOTCH1*, *TP53*, and *SF3B1*); (b) clonally represented in CLL and absent in the paired RS (data based on CN, FISH and WES analyses); and (c) acquired in the CLL-RS transition (data based on CN, FISH and WES analyses). In three cases (on the right portion of the graph), the terminal leukemic phase of RS (RSII) was included in the analysis (cases 2, 4, and 5). In case 5, the acquired lesions are based on WES and FISH data; none of the discovery cases carried mutations shared between CLL and RS in the *ATM* and *MYD88* genes. Tx, translocation; M, mutation.

phase and in all following RS biopsies; a homozygous frame-shift deletion in the *SPEN* gene (P1356fs), a putative negative regulator of NOTCH signaling targeted by inactivating mutations in splenic marginal zone lymphoma (Kuroda et al., 2003; Saito et al., 2003; Rossi et al., 2012c), was acquired at RS diagnosis and maintained in the leukemic phase of the disease; and during the progression from nodal localization (RS) to peripheral blood invasion (RSII), a second *NOTCH1* mutation targeting the heterodimerization domain of the protein was acquired (V1721M; Fig. 3, c and d). The detection of PEST and heterodimerization domain mutations in the same patient is of relevance, as mutations in these two distinct domains have been shown to act synergistically in promoting signaling activation (Weng et al., 2004).

Overall, these patterns of somatic alterations are consistent with a predominantly linear evolutionary model, in which RS evolves through the addition of novel genetic lesions to those already present in the predominant CLL clone. In contrast, the blood localization of the disease seems to be often the result of a branching pattern of evolution, consistent with the selection and expansion of an ancestral precursor clone that was present in the patients at an earlier stage than the time of the initial diagnostic RS biopsy (Fig. 2).

RS acquires a heterogeneous number and spectrum of genetic lesions

To assess the load and the spectrum of genetic lesions acquired in the transition of CLL to RS, we next focused on the set of genetic aberrations present exclusively in the RS coding genome. WES analysis in the 9 CLL-RS pairs revealed the presence of 241 nonsilent mutations specific for RS, either at diagnosis ($n = 165$, range 0–118 events/case) or in the terminal leukemic phase of the disease ($n = 76$, range 0–36 events/case; Table S2; Fig. 1 c). A subset of these mutations ($n = 13/241$, 5.4%) was already detectable in a small fraction of the CLL sequencing reads (≤20%), suggesting their presence at the subclonal level early during CLL development, and subsequent selection and outgrowth during transformation. Analogously, CN analysis of the same cases, and of the 6 pairs with only CN data available, revealed the presence of 138 CNAs specific for RS at diagnosis ($n = 95$, range 0–29/case) or for the terminal leukemic phase ($n = 43$, range 14–29; Table S3; Fig. 1 c).

The combination of WES, CN, and FISH data obtained in the 9 pairs for which the complete set of analysis was available showed that the RS genome acquires a mean of ∼22 genetic lesions/case, with a great variability across individual
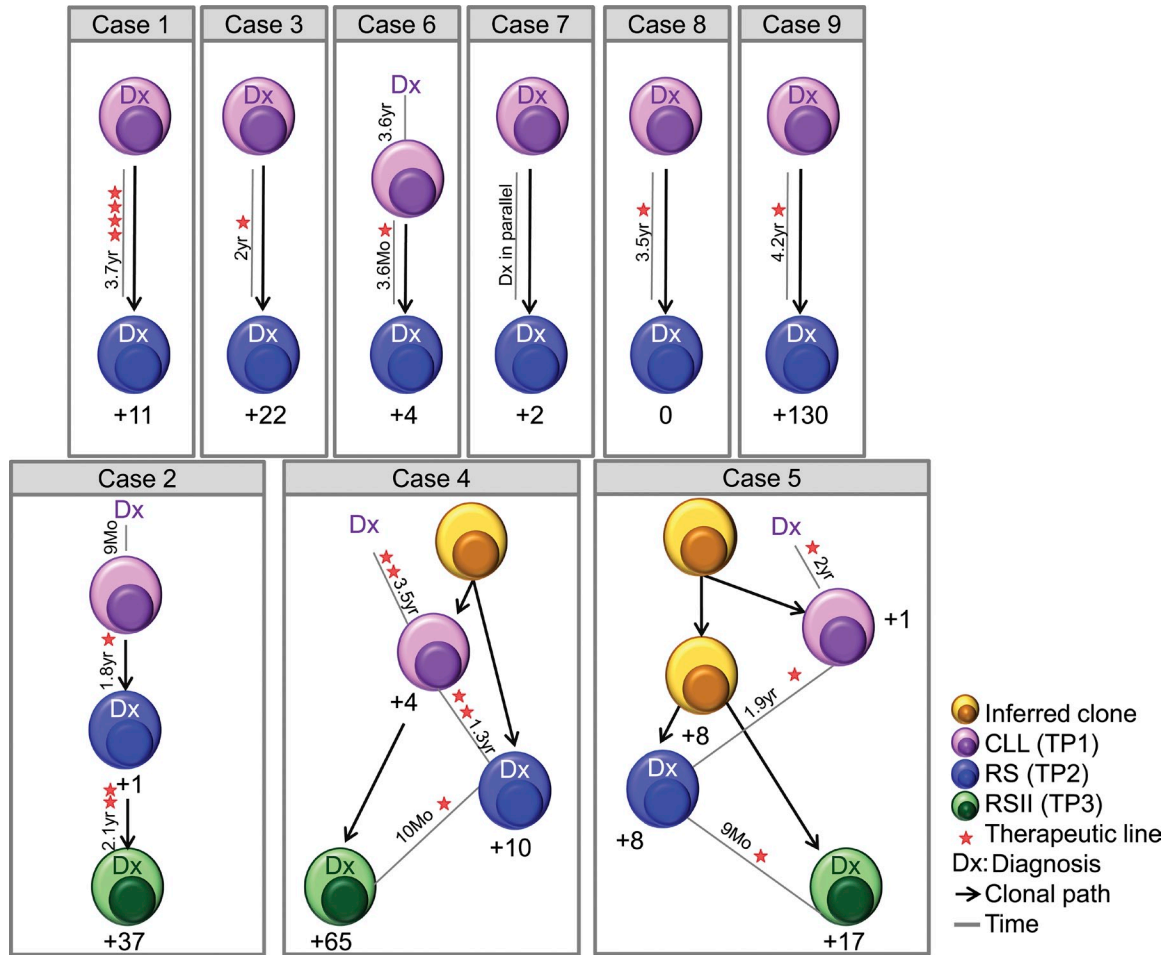
Figure 2.   Patterns of genetic evolution of CLL to RS. In each case the analyzed CLL clone is represented by a purple cell, the RS clone by a blue cell, and the RSII clone by a green cell (available in cases 2–4–5). Inferred clones are represented in orange. Bold black arrows depict the clonal path between samples and the time elapsed between samples is highlighted next to the gray lines interconnecting the analyzed time points. Each therapeutic line administered to patients is represented by a red star. The number of genetic lesions acquired in the CLL-RS transition is highlighted below the RS or RSII clone, respectively. TP, time-point; yr, years; Mo, months.

samples (range 0–130/case; Fig. 1 c). The only case (8-RS) in which we did not detect any RS–specific genetic lesion may have acquired genetic/epigenetic aberrations not assessable with our integrated approach (e.g., translocations, mutations in noncoding regulatory portions of the genome, or aberrant methylation; Küppers and Dalla-Favera, 2001; Kulis et al., 2012; Huang et al., 2013). The lack of acquisition of lesions in this patient was not caused by low tumor representation, as documented by the presence of a set of abnormalities, including a *TP53* mutation, which were shared by the CLL and RS phase (Fig. 1 a). The load of alterations acquired by the terminal leukemic phase of the disease was higher compared with the one observed in the CLL-RS transition, with ∼40 acquired lesions per case on average (Fig. 1 c).

Although the number of cases studied is limited, no significant difference in the load of acquired genetic lesions was observed between *IGHV* mutated or unmutated RS or in cases with different clinical stages of the disease (Fig.1; Table S1).

A detailed list of genes altered in RS in the discovery panel is reported in Tables S2 and S3, with notes on their possible functional significance.

Overall, these data show that the genetic lesions acquired in the transition of CLL to RS are quite heterogeneous in terms of load and spectrum across samples.

Recurrent targets of CN changes in RS: frequent loss of *TP53* and *CDKN2A/B*

One way to determine the relevance of newly identified genetic lesions is to assess their recurrence in the disease. Toward this end, we first extended the CN analysis to a larger cohort of RS ($n = 42$ cases). Consistent with the results obtained in the discovery panel, this analysis confirmed the high degree of heterogeneity of the RS genome, with on average ∼12.5 CNAs per case and a range of 0–55 aberrations per sample, mostly represented by CN losses, which accounted for ∼60% of the identified lesions (Fig. 4 a).
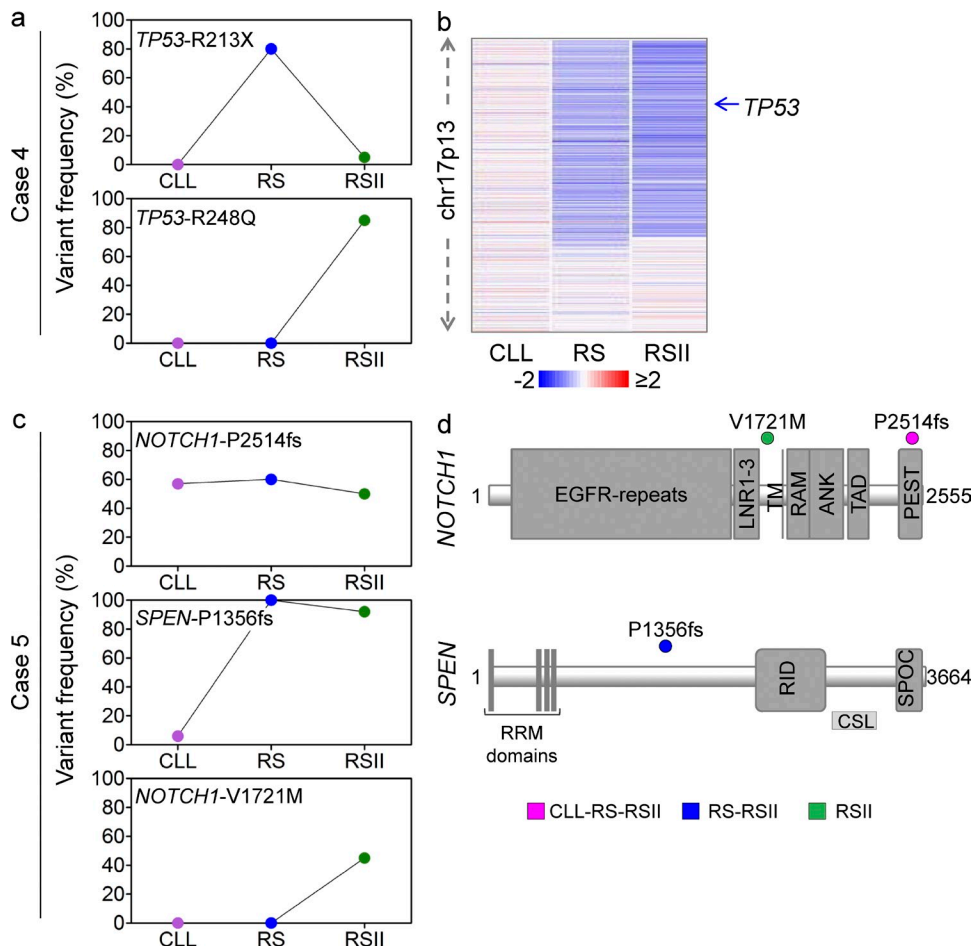
**Figure 3. Representative examples of clonal evolution of genetic lesions during CLL transformation to RS and subsequent RS progression.** (a and b) Different tumor clones acquire biallelic *TP53* disruption in RS and RSII in case 4. (a) Graphs reporting the variants' adjusted frequencies as identified by WES analysis in the *TP53* gene in the CLL, RS, and RSII phases of case 4. (b) Heatmap showing median-smoothed log2 CN ratio of the short arm of chromosome 17 in the CLL, RS, and RSII phases of case 4. (c and d) Progressive accumulation of multiple genetic lesions leading to NOTCH signaling activation in case 5. (c) Graphs reporting the variants' adjusted frequencies as identified by WES analysis in the *NOTCH1* and *SPEN* genes in the CLL, RS, and RSII phases of case 5. (d) Schematic of mutations affecting *NOTCH1* and *SPEN* in the CLL, RS, and RSII phases of case 5.

We identified 107 focal minimal common regions (MCRs) of aberration (84 of loss and 23 of gain) encompassing 1–3 protein-coding genes, which most likely represent the target of the lesion (Fig. 4 b). The relevance of the identified lesions was confirmed through GISTIC, an algorithm based on the amplitude and frequency of occurrence of CN changes (Beroukhim et al., 2007; Fig. 4 d). To address the specificity of these newly identified recurrent regions of CN aberration for RS, we compared their frequency with that reported in a cohort of 353 newly diagnosed and previously untreated CLL cases (Edelmann et al., 2012), focusing on genes altered in ≥10% of RS cases as well as on known recurrent cytogenetic abnormalities (Edelmann et al., 2012; Fig. 4, b and c).

Consistent with previous reports (Rossi et al., 2011b), the most frequent aberration significantly enriched in RS was represented by del17p, detected in ∼40% of RS cases and in the majority of the cases involving the *TP53* tumor suppressor gene (*n* = 18/20). Notably, the overall number of genetic

lesions was significantly higher in *TP53*-disrupted cases compared with *TP53* wild-type cases, consistent with an increased genomic instability caused by this genetic abnormality (P < 0.001; Fig. 4 e; Ouillette et al., 2010). Moreover, four *TP53* disrupted cases displayed complex intrachromosomal rearrangements caused by alternating gains and losses of genetic material, frequently accounting for >10 switches per chromosome, possibly suggestive of chromothripsis (unpublished data). A preferential association of this phenomenon with *TP53* lesions has been reported in CLL (Edelmann et al., 2012), as well as in other tumor types such as medulloblastoma (Rausch et al., 2012).

Our analysis identified del9p21 as a frequent genetic aberration commonly detectable in RS (∼30% of cases) and shown to be specifically acquired at transformation in all cases in which the CLL phase was available (*n* = 3/3; Fig. 5, a and b). Consistently, del9p21 was never observed in unselected CLL cases (Edelmann et al., 2012). In seven out of the 15 affected
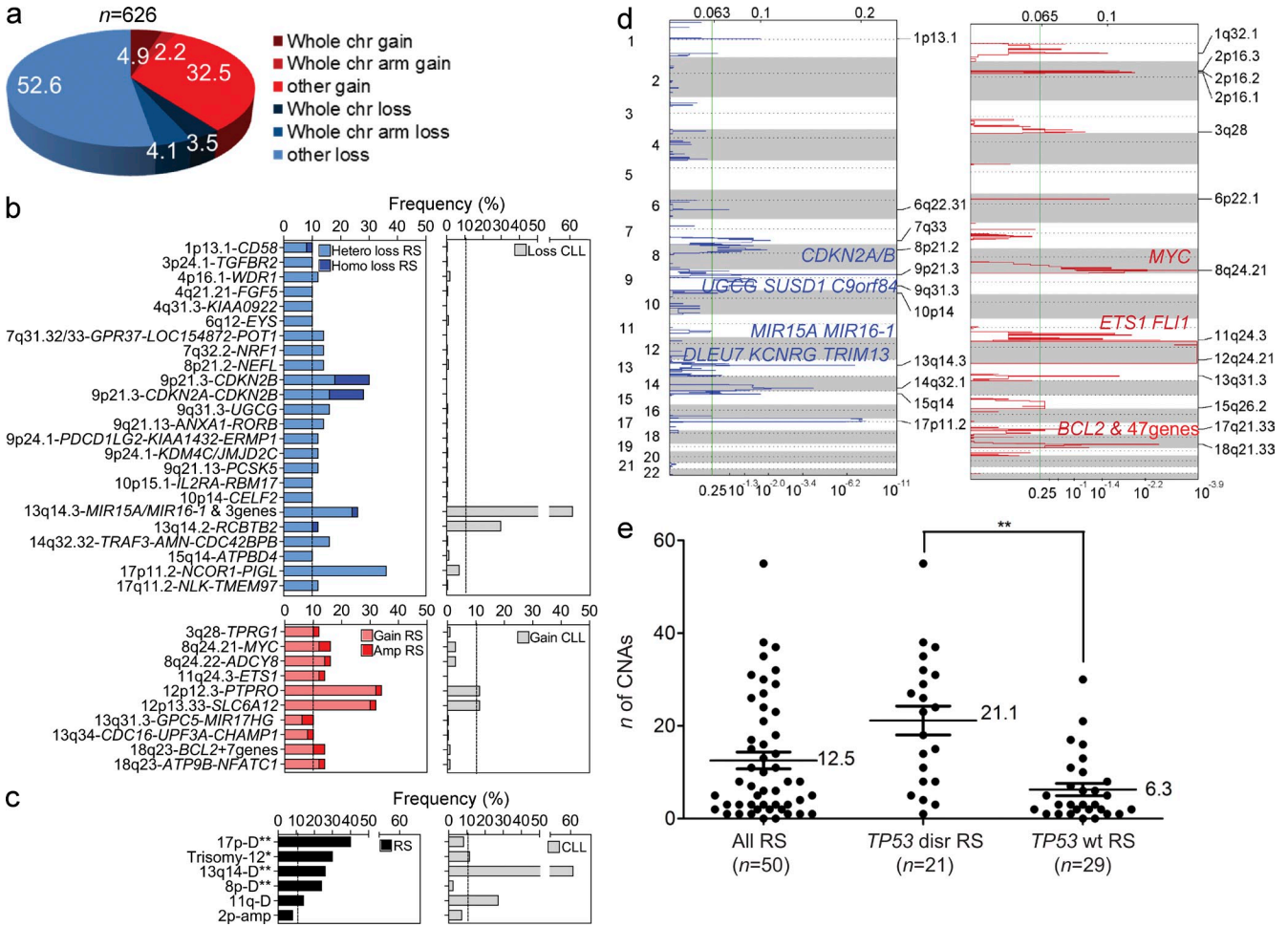
Figure 4. **Overall picture of CNAs in the RS coding genome.** (a) Overall number and frequency of CNAs in RS. (b) Minimal common regions (MCRs) of CN loss (top) or CN gain (bottom) encompassing 1–3 protein-coding genes and altered in ≥10% of RS cases (n = 50; blue and red bars), ranked by chromosome and frequency of alteration. Gray bars represent the frequency of loss (top) or gain (bottom) affecting the genes included in the annotated MCR in a series of 353 CLL cases as reported in Edelmann et al. (2012). All reported MCRs occurred with a significantly different frequency between CLL and RS based on a two-tailed Fisher's exact test (all with P < 0.001). (c) Frequency of known CLL-associated cytogenetic abnormalities in RS (n = 50 cases, black bars) and in a series of 353 CLL cases as reported in Edelmann et al., 2012 (gray bars). Asterisks indicate lesions present with different frequency between CLL and RS based on a two-tailed Fisher's exact test (*, P < 0.05; **, P < 0.001). (d) Statistical analysis of CN losses (left, blue) and gains (right, red) in 50 RS cases according to GISTIC. False discovery rates for each aberration (q values, x axis) are plotted at each genomic position across chromosomes 1–22 (y axis). The green line represents the q value cutoff for significance (0.25). Centromere positions in each chromosome are indicated by dotted lines, and the gene names are provided only for focal aberrations encompassing ≤3 genes, unless indicated. (e) Distribution of the total number of CNAs in 50 RS cases (all or grouped according to the presence or absence of TP53 disruption). **, P < 0.001 according to a nonparametric two-tailed Student's t test.

cases (46.7%), the loss of genetic material encompassed <10 genes, always including the *CDKN2A/B* locus. Disruption of *CDKN2A/B* was biallelic in over one third of cases (n = 6/15); in 3 of them, this was a result of reduplication of 1 allele carrying a hemizygous *CDKN2A/B* deletion, as assessed by LOH analysis, whereas one additional case harbored a heterozygous deletion with a *CDKN2A* splice site mutation in the second allele (Fig. 5 c and Table S2). One patient (16-RS) harbored a focal CN loss encompassing only the *CDKN2B* gene, which encodes for p15INK4B, a regulator of cell cycle arrest that is potently induced by TGF-β signaling (Hannon and Beach, 1994). Collectively, these results suggest that the

CDKN2A/B locus is the specific target of the 9p21 deletions, which is consistent with observations in other tumor types (Sherr, 2004).

CDKN2A encodes both for the negative regulator of cell cycle p16INK4A (Serrano et al., 1993) and for ARF, an inhibitor of the negative regulator of p53 MDM2 (Zhang et al., 1998). We thus sought to analyze the distribution of aberrations involving this locus with other lesions known to affect key regulators of cell cycle control and DNA repair (Fig. 5 d). This analysis revealed that *CDKN2A* losses, *TP53* disruption, and *MYC*-activating events often coexist. Interestingly, all these lesions were mutually exclusive with trisomy 12, another
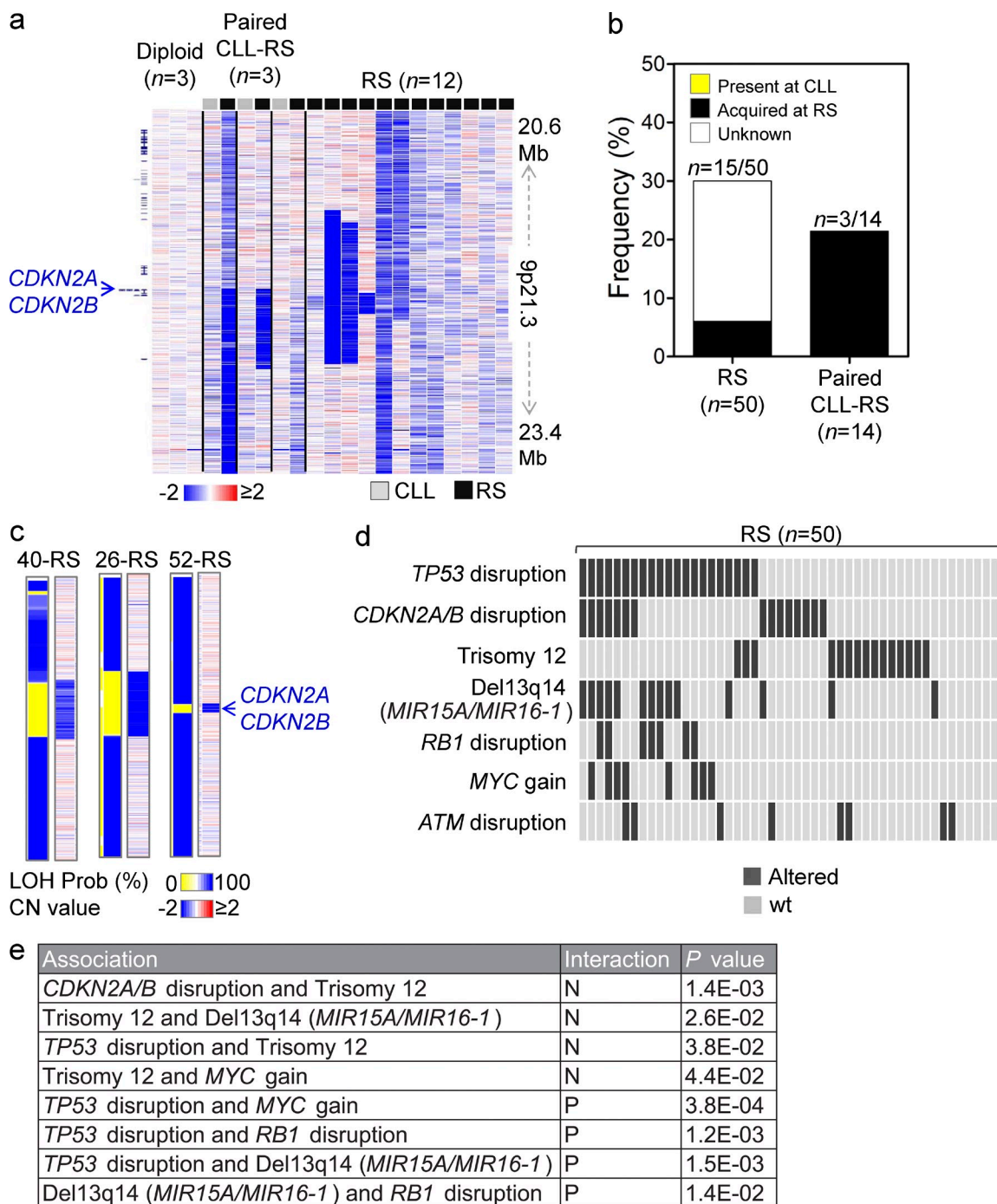
Figure 5. Loss of 9p is commonly acquired in RS. (a) dChip inferred CN heat map showing the magnification of deletions affecting the *CDKN2A/B* locus on chromosome 9 in the RS samples carrying the loss (three with paired CLL). The first three columns represent normal (diploid) samples. In the red-blue scale, white corresponds to a normal (diploid) CN log2-ratio, blue to deletion, and red to gain. (b) Percentage of RS samples harboring *CDKN2A/B* deletions. (c) Regions of copy-neutral LOH affecting the *CDKN2A/B* locus. The left-side shows the inferred probability of LOH for each case, which is displayed from blue (1) to white (0.5) to yellow (0), and the right side shows a heatmap of the median-smoothed log2 CN ratio of the locus (blue is deletion and red is gain). (d) In the heatmap, rows correspond to the indicated aberrations and columns represent individual RS samples, color-coded based on the gene status (light grey, wild-type; dark grey, altered). (e) Significant associations between genetic lesions are listed with their corresponding p-value. Prob, probability; N, mutual exclusion; P, positive association.

recurrent alteration observed in ~30% of RS cases (P < 0.05). In addition, *TP53* disruption was significantly (P < 0.05) associated with del13q14 and with *RB1* disruption (Fig. 5 e).

Several additional CN changes occurred at higher frequency in RS compared with CLL, including trisomy 12, losses of the 7q31.31–36.3, 8p and 14q23.2-q32.33 loci, and

high level amplifications affecting the long arm of chromosomes 8, 11, 13, and 18. The putative targets of these lesions included genes previously linked to cancer, such as *POT1*, a gene involved in telomeres protection, which was reported to harbor mutations in ~3% of CLL patients and also found to be mutated in 2 of our 27 RS (Table S2; Baumann and Cech, 2001; Quesada et al., 2012; Landau et al., 2013; Ramsay et al., 2013); *TRAF3*, a negative regulator of noncanonical NF-κB that is frequently inactivated in multiple myeloma (Annunziata et al., 2007; Keats et al., 2007); and the oncogenes *MYC*, *ETS1*, *MIR17HG*, and *BCL2* (Vaux et al., 1988; Bories et al., 1995; He et al., 2005; Xiao et al., 2008). No point mutations were found in the aforementioned genes.

Among the other CNAs that are recurrent in CLL patients, del11q and gains of the 2p16.1–2p15 locus occurred in RS at a frequency comparable to that of unselected CLLs (14 and 8% vs. 27 and 7%, respectively; Fig. 4 c; Edelmann et al., 2012). In contrast, the frequency of del13q14 was significantly lower in RS compared to CLL cases at diagnosis (~28 vs. 61%; P < 0.001), consistent with the observation that its absence is an independent risk factor for RS development and that this lesion, known to be an early event in CLL onset, was never acquired at RS (Edelmann et al., 2012; Rossi et al., 2008).

Collectively, these results confirm the high degree of heterogeneity of the RS genome, point to relevant genes and loci not previously linked to RS, and provide a large array of novel candidates for mutational analysis.

Recurrent targets of point mutations in RS

To identify recurrent targets of point mutations in RS, we performed WES analysis in a "screening panel" of 18 RS cases. Due to the unavailability of paired normal DNAs, the mutation frequency was only assessed on those genes/mutations for which previous information of functional relevance was available, including: (a) genes identified by WES in the discovery panel ($n = 231$); (b) genes located in the focal MCR of an aberration with a frequency ≥10% ($n = 54$); and (c) genes mutated in de novo DLBCL and CLL, as identified in recently published genome-wide studies (Fabbri et al., 2011; Morin et al., 2011; Pasqualucci et al., 2011; Puente et al., 2011; Wang et al., 2011; Lohr et al., 2012; Quesada et al., 2012; Landau et al., 2013) and listed in the Cancer Gene Census or for which mutations have been implicated functionally in cancer ($n = 215$). Using these criteria, we interrogated a total number of 481 genes. Fig. 6 shows the prevalence (including discovery and screening panels) of RS cases with mutations in genes altered with a frequency >10% ($n = 23$).

To address the specificity of the newly identified recurrent mutations for RS, we compared their frequency with the one previously reported in whole-exome/genome studies performed in CLL patients ($n = 205$; Fabbri et al., 2011; Puente et al., 2011; Quesada et al., 2012; Wang et al., 2011). Indeed, with the exception of three genes previously linked to CLL (i.e., *MYD88*, *SF3B1*, and *ATM*; Stankovic et al., 1999; Wang et al., 2011; Puente et al., 2011; Quesada et al., 2012), 20/23 mutated genes were altered at a significantly

higher frequency in RS (p-values in Fig. 6) compared with CLL. This finding is consistent with the notion that *MYD88* mutations seem to arise early in the natural history of CLL (Landau et al., 2013) and with the reported enrichment of *SF3B1* mutations, which often coexist with *ATM* disruption (Wang et al., 2011) in CLL cases refractory to fludarabine-based therapy compared with CLLs at diagnosis and RS patients (Rossi et al., 2011a).

Genes affected in >10% of RS patients were representative of a variety of biological programs, including DNA repair (*TP53* and *ATM*; Stankovic et al., 1999; Zenz et al., 2010), NOTCH signaling pathway (*NOTCH1* and *SPEN*; Fabbri et al., 2011; Puente et al., 2011; Rossi et al., 2012c; Saito et al., 2003), transcription and chromatin remodeling (*ZFHX3*, *ARID1A*, *ARID1B*, *MLL2*, and *IRX5*; Sun et al., 2005; Grasso et al., 2012; Wu and Roberts, 2013), B cell development/activation (*IRF8*, *PIM1*, and *MYD88*; Domen et al., 1993; Wang and Morse, 2009; Rawlings et al., 2012), PI3K pathway (*PREX2*; Berger et al., 2012; Fine et al., 2009), cytoskeleton/extracellular matrix organization and adhesion (*PCLO*, *COL27A1*, *COL2A1*, *SVEP1*, and *SYNE2)*, ubiquitin proteolysis (*USP8*, *USP34*; Berlin et al., 2010; Lui et al., 2011), and splicing regulation (*SF3B1*; Golas et al., 2003; Fig. 6). A detailed description of the identified mutations is reported in Table S2, with remarks on their possible functional consequence. Overall, these data point to specific oncogenic biological programs and pathways involved in the pathogenesis of the disease, as described in the following section.

Cellular programs commonly altered in RS

To organize the spectrum of genetic lesions in cellular pathways relevant for RS pathogenesis, we performed pathways/gene functional clustering analysis using an integrated approach based on the combination of publicly available tools (i.e., GSEA and DAVID 2008; Mootha et al., 2003; Subramanian et al., 2005; Huang et al., 2009a,b) and manual annotation of the genes altered in RS, including (a) RS-WES mutated genes; (b) genes in focal MCR of aberration with a frequency ≥10%; and (c) "de novo DLBCL/CLL CGC genes" mutated in at least 2 RS cases (total $n = 304$ genes).

All used tools reported proliferation-, apoptosis-, and cell–cycle regulation in the top statistically significant categories, suggesting that deregulation of these processes is the driving force of this highly aggressive tumor that combines in a single disease the effects of chemoresistance and rapid disease kinetics. Based on our integrated analysis, the four genes most commonly altered in RS were *TP53*, *NOTCH1*, *MYC*, and *CDKN2A/B*, which are well-characterized regulators of tumor suppression, cell proliferation, and cell cycle control, whose lesions overall accounted for ~90% of RS cases (Figs. 6–8). Additional programs and pathways that emerged as significantly altered in RS included the MAPK, Wnt, NF-κB, and TGF-β pathways, RNA processing/degradation, and protein translation processes.

Collectively, these results suggest that the transformation of CLL to RS involves a heterogeneous set of pathways in
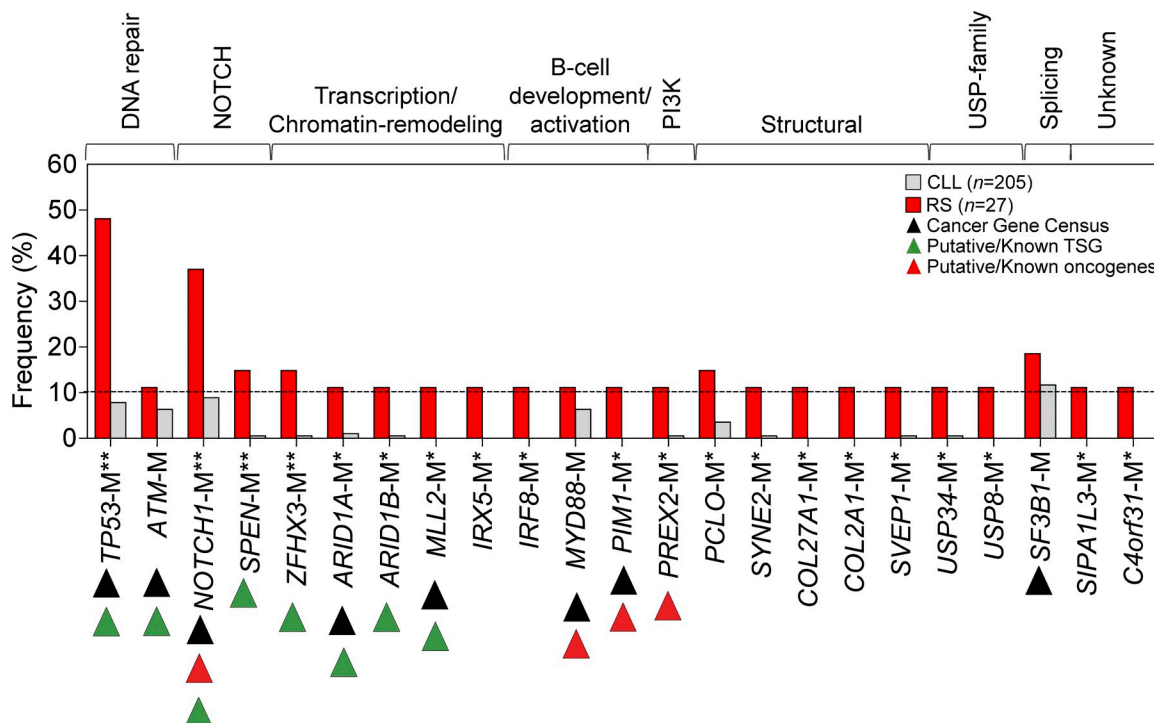
Figure 6. Genes recurrently mutated in RS. Percentage of RS cases (*n* = 27) harboring mutations in genes altered with a frequency >10% (red bars). The mutation frequency of these genes in CLL (gray bar) was obtained in a dataset of 205 CLL cases analyzed for whole-exome/whole genome sequencing (see main text). Asterisks indicate genes differentially mutated between CLL and RS based on a two-tailed Fisher's exact test (*, P ≤ 0.05; **, P ≤ 0.001). Black triangles denote genes reported in the Cancer Gene Census database (http://www.sanger.ac.uk/genetics/CGP/Census/); green triangles indicate putative or proven tumor suppressor genes; and red triangles denote putative or proven oncogenes. TSG, tumor-suppressor gene; ns, not significant.

different cases, with those involving apoptosis and cell proliferation representing the most consistent ones.

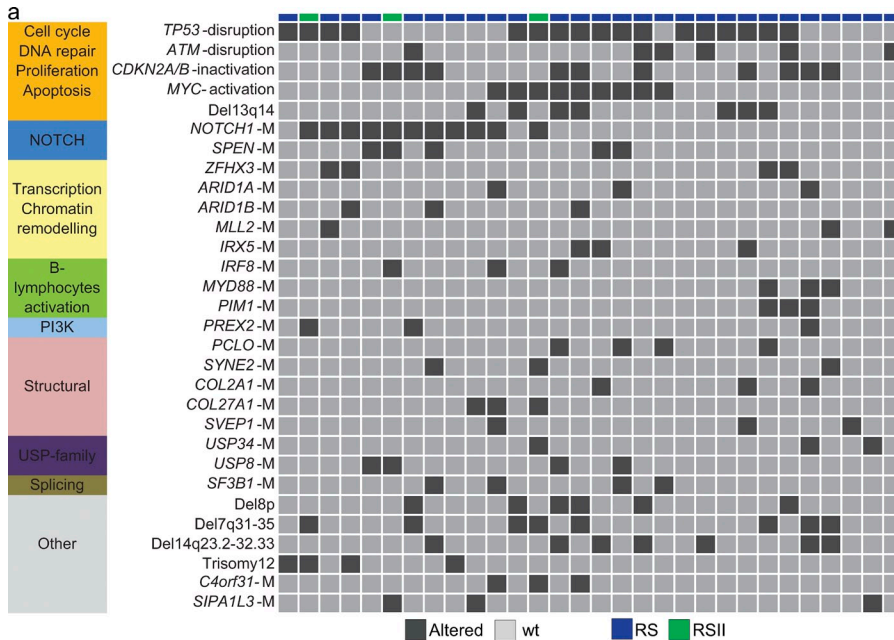## The coding genome of RS is distinct from the one of de novo DLBCL

Although most RS cases are histologically classified as DLBCL, the response to treatment is significantly poorer in RS than in de novo DLBCL, even when considering the less curable activated B cell–like subtype (Coiffier et al., 2002; Tsimberidou et al., 2006; Tsimberidou et al., 2008), suggesting a distinct underlying pathogenesis. To obtain a comparative assessment of the genetic landscape of these two diseases, we compared the frequency of the most prevalent genetic lesions in 27 RS cases, characterized for WES and CN data (see above), and in 71 newly diagnosed and previously untreated DLBCL cases, with available CN and targeted resequencing data of genes commonly mutated in DLBCL (Pasqualucci et al., 2011). We separately compared the frequency of genetic lesions in RS versus the two main subtypes of DLBCL, i.e., activated B cell–like (ABC, *n* = 40) and germinal center B cell like (GCB, *n* = 31) DLBCL (Fig. 8). For genes for which we lacked mutational analysis data, we used a recently published WES-dataset of 49 primary DLBCL cases with no information regarding ABC versus GCB subtype (Lohr et al., 2012).

Although almost all RS cases display a nongerminal center phenotype (Hans et al., 2004), the genetics of RS significantly differed from that of de novo ABC-DLBCL, with the exception of *CDKN2A/B* losses and point mutations affecting *MYD88*, which were, overall, observed at comparable frequency. In particular, several lesions typically associated with ABC-DLBCL were rare or absent in RS. Significant differences included biallelic inactivation of the *TNFAIP3/A20* and *PRDM1/BLIMP1* tumor suppressor genes and *BCL6* translocations, which were never observed in RS, whereas they are associated with ∼30, ∼22, and 37.5% of ABC-DLBCL, respectively (P < 0.01; Fig. 8). Additional lesions typically associated with ABC-DLBCL, including mutations of *PIM1*, *CD79B*, and *CARD11*, as well as *BCL2*-CN gains, were relatively rare in RS (11.1 vs. 17.5%, 7.4 vs. 25%, 7.4 vs. 12.5%, and 22.2 vs. 42.5%, respectively).

Among the lesions typically associated with GCB-DLBCL, *MYC*-activating events presented comparable frequencies in the two diseases (Fig. 8), whereas mutations involving *CREBBP* and *EZH2,* which were observed in 22.6 and 9.7% of GCB-DLBCL, respectively, never occurred in RS. The difference was statistically significant (P < 0.05) only for *CREBPP* mutations, most likely due to the lower frequency of *EZH2* mutations in GCB-DLBCL. *BCL2* translocations, present in ∼30% of GCB-DLBCL, were never observed in RS, as previously reported (Rossi et al., 2011b; P < 0.01).

Finally, among the lesions equally represented in both DLBCL subtypes, some occurred with similar frequency in

a

Cell cycle
DNA repair
Proliferation
Apoptosis

NOTCH

Transcription
Chromatin
remodelling

B-
lymphocytes
activation

PI3K

Structural

USP-family

Splicing

Other

TP53-disruption
ATM-disruption
CDKN2A/B-inactivation
MYC-activation
Del13q14
NOTCH1-M
SPEN-M
ZFHX3-M
ARID1A-M
ARID1B-M
MLL2-M
IRX5-M
IRF8-M
MYD88-M
PIM1-M
PREX2-M
PCLO-M
SYNE2-M
COL2A1-M
COL27A1-M
SVEP1-M
USP34-M
USP8-M
SF3B1-M
Del8p
Del7q31-35
Del14q23.2-32.33
Trisomy12
C4orf31-M
SIPA1L3-M

▮ Altered ▮ wt ▮ RS ▮ RSII

Figure 7. Distribution of recurrent genetic lesions among RS cases. (a) In the heatmap, rows correspond to the indicated genetic lesions, and columns represent individual RS or RSII samples, color-coded based on the gene status (light gray, wild-type; dark gray, mutated or activated or disrupted). (b) Significant associations are listed with their corresponding p-value. N, mutual exclusion; P, positive association. This figure displays only the 27 RS cases characterized by WES analysis. Therefore, some of the associations and anti-correlations shown in Fig. 5 may not reach statistical significance due to the lower number of cases.

b

Association	Interaction	P value
MYD88-M and Del7q31-35	P	1.20E-02
PREX2-M and Del7q31-35	P	1.20E-02
IRX5-M and COL2A1-M	P	2.50E-02
IRF8-M and USP8-M	P	2.50E-02
MYD88-M and PIM1-M	P	2.50E-02
COL27A1-M and C4orf31-M	P	2.50E-02
MYC-activation and C4orf31-M	P	2.87E-02

Association	Interaction	P value
NOTCH1-M and COL27A1-M	P	4.10E-02
NOTCH1-M and Trisomy12	P	4.10E-02
SPEN-M and USP8-M	P	4.85E-02
ZFHX3-M and PIM1-M	P	4.85E-02
ARID1A-M and SF3B1-M	P	4.85E-02
PCLO-M and USP8-M	P	4.85E-02

the two diseases (i.e., *MIR17HG* gain, 8p loss, and deletion of *PTEN*). *B2M* biallelic disruption and gains of chromosome 7 occurred less frequently in RS compared with DLBCL (0 vs. 16.9%, and 7.4 vs. 38%, respectively; P < 0.05). The frequency of *MLL2* and *PCLO* mutations was also lower in RS compared with DLBCL (15 vs. 35% and 11.1 vs. 22.5%), but this difference did not reach statistical significance (Fig. 8). Strikingly, the two most frequent genetic lesions that characterize the RS genome, i.e., *TP53* biallelic disruption and *NOTCH1* mutations, were significantly enriched in RS compared with both subtypes of DLBCL (P < 0.01), thus confirming their specific relevance in the pathogenesis of the disease (Fig. 8).

Altogether, these data underline the fact that, despite the morphological and phenotypic similarities between RS and de novo DLBCL, the molecular profile of these two conditions is largely different, suggesting that they represent distinct disease entities.

DISCUSSION

This study was aimed at elucidating relevant questions regarding RS pathogenesis, including its pattern of clonal evolution from CLL, the genetic determinants of the transformation event, and the pathogenetic relationship between RS and classical non-CLL associated de novo DLBCL. Although these questions have been previously addressed using mostly candidate gene approaches, we have used unbiased whole-exome and CN analysis for a comprehensive definition of these issues.

The obtained results provide insights into RS pathogenesis and have diagnostic and therapeutic implications.

The clonal evolution of any given tumor type occurs either through a linear model, in which the predominant clone acquires novel genetic lesions leading to progression, or a branching model, in which a common ancestor evolves to the initial tumor and to the progressed stage through distinct genetic pathways (Aparicio and Caldas, 2013). Our results show that the CLL-RS transition occurs through a linear model of evolution in most cases, where RS represents the final stage of evolution of the original founder CLL clone. This result is consistent with early observations based on the analysis of intraclonal diversification of *IGHV* genes in paired CLL-RS (Rossi et al., 2012b). In a minor fraction of cases, RS seems to be the result of the branching evolution of CLL and RS from an earlier common precursor cell, perhaps consistent with the observation that early hematopoietic stem cells from CLL patients can acquire propensity to generate clonal B cells (Kikushige et al., 2011). Both linear and branching patterns of clonal evolution have been described in CLL clinical progression (Schuh et al., 2012; Landau et al., 2013; Ouillette et al., 2013), as well as in the transformation of follicular-lymphoma (FL) to DLBCL (Carlotti et al., 2009; and unpublished data), although in the latter case a branching pattern of evolution is predominant. This is also the case in the rare progression of RS from a nodal to a leukemic disease, at least in two out of the three cases analyzed in this study. The terminal leukemic phase of RS might be the result of the selection and outgrowth of a subclone, perhaps driven by
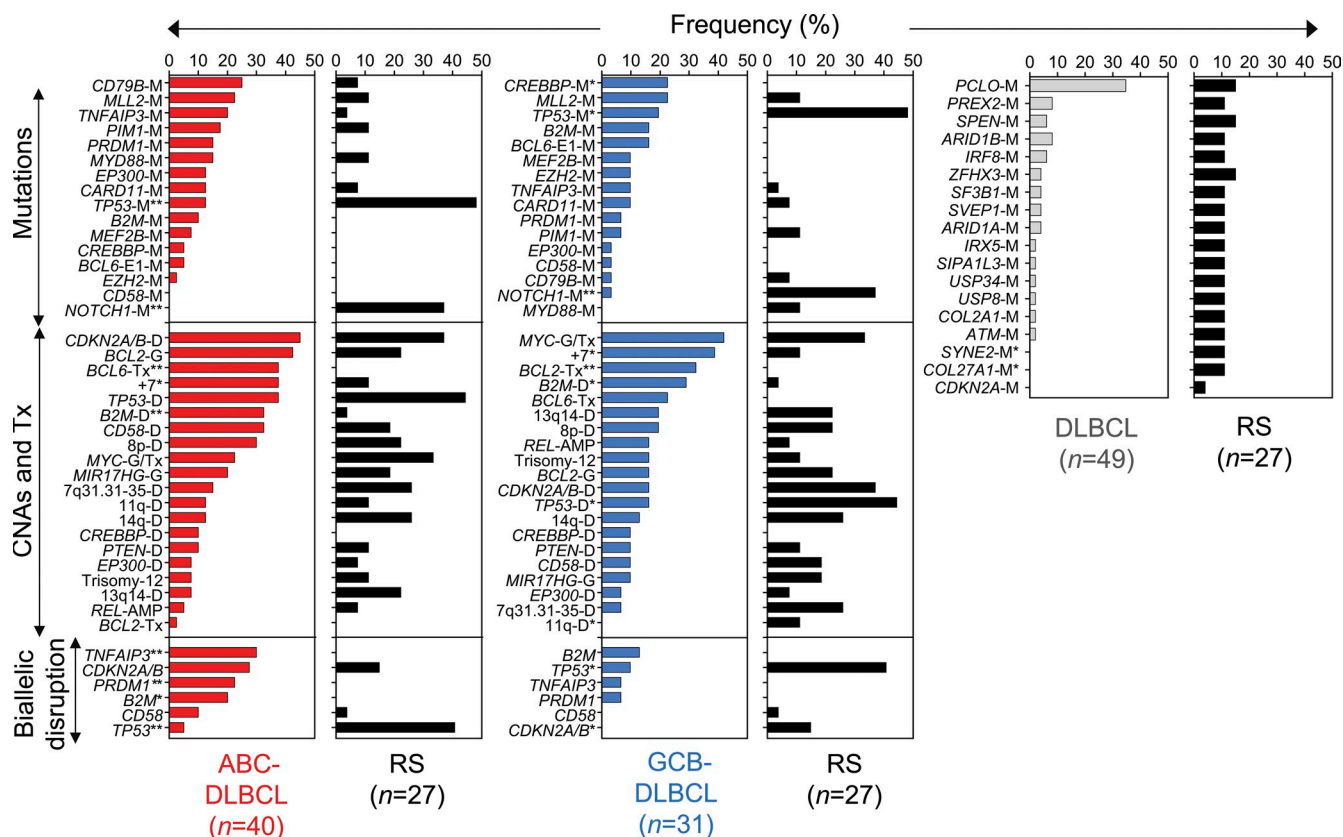
Figure 8. The genetic profile of RS differs from that of de novo DLBCL. Percentage of de novo DLBCL and RS cases carrying genetic lesions typically associated with de novo DLBCL and/or RS. The RS panel was composed of 27 cases characterized by WES and CN data (black bars). The de novo DLBCL panel was composed of 71 newly diagnosed and previously untreated DLBCL cases (ABC, n = 40, red; GCB, n = 31, blue), with available CN data and targeted resequencing data of genes commonly mutated in de novo DLBCL. For genes for which we lacked mutational analysis data, we used a recently published WES-dataset of 49 primary DLBCL cases as reported in Lohr et al. (2012; gray bars). Asterisks indicate genes differentially mutated between RS and de novo DLBCL (two-tailed Fisher's exact test; *, P < 0.05; **, P < 0.01). CNAs, CN aberrations; D, deletion; G, gain; AMP, amplification; Tx, translocation. Biallelic disruption includes M/M, M/D, and D/D events.

the highly cytotoxic therapeutic regimes used for RS treatment (Rossi and Gaidano, 2009).

Moreover, our data reveal that no single lesion or combination of genetic lesions or cellular pathways seem to be responsible for CLL transformation to RS, with various RS cases differing in both the number and the type of aberrations. Nonetheless, the fact that ~90% of the cases display combinations of lesions of *TP53*, *NOTCH1*, *MYC*, and *CDKN2A/B* suggests that RS transformation does not involve primarily specific B cell signaling pathways, but rather general regulators of tumor suppression, cell cycle control and cell proliferation. Whereas previous reports have already identified *TP53* inactivation, and the mutually exclusive *NOTCH1* and *MYC*-activating events as common in RS pathogenesis (Fabbri et al., 2011; Rossi et al., 2011b), our results identify loss of the *CDKN2A/B* locus as present in ~30% of RS cases and often co-occurring with the two other most frequent lesions observed in RS, namely *TP53* disruption and *NOTCH1* mutations. The individual and combined role of these lesions can be studied further in appropriate mouse models. Overall, we note that RS transformation

appears to involve pathways that are distinct from those accompanying CLL progression and/or acquisition of chemoresistance, the latter being recurrently associated with lesions of the *SF3B1* gene, encoding a component of the spliceosome, and of the *BIRC3* gene, encoding a negative regulator of the NF-κB pathway, although largely lacking *MYC* activation and *CDKN2A/B* disruption that are common in RS (Wang et al., 2011; Quesada et al., 2012; Rossi et al., 2011a,b).

The results herein also indicate that the DLBCL disease typical of RS is pathogenetically distinct from both forms (GCB and ABC) of de novo DLBCL (Morin et al., 2011; Pasqualucci et al., 2011). The most relevant differences involve the common activation of NOTCH and inactivation of TP53 pathways, which are virtually absent or rare in de novo DLBCL, respectively. Furthermore, RS-DLBCL lacks lesions common in all DLBCL types, such as inactivation of the acetyltransferase genes *CREBBP/EP300* and of the *B2M* gene, as well as those common in ABC-DLBCL (e.g., translocations of *BCL6* and loss of *PRDM1/BLIMP1* and *TNFAIP3/A20*) or GCB-DLBCL (e.g., translocations of *BCL2*; Challa-Malladi

et al., 2011; Lohr et al., 2012; Morin et al., 2011; Pasqualucci et al., 2011). These differences indicate that DLBCL transformed from CLL and classical DLBCL represent distinct disease entities.

Finally, these findings have diagnostic and therapeutic implications. The higher frequency of specific lesions in RS compared with CLL suggests that their early detection can be tested for its prognostic significance in predicting CLL evolution toward RS. Moreover, the specific presence (e.g., *NOTCH1* mutations) or absence (e.g., inactivation of *CREBBP/EP300* and translocations of *BCL2*) of defined lesions in RS imply distinct approaches in identifying targeted therapies from those currently being tested for DLBCL. In particular, two of the most common lesions occurring in RS, namely *NOTCH1* mutations and *CDKN2A/B* deletions, represent established therapeutic targets with some drugs being already available for testing in single or combinatorial regimens (Monti et al., 2012; Samon et al., 2012; Wu et al., 2010).

MATERIALS AND METHODS

Primary cases. The discovery panel comprised 21 samples from 9 paired CLL-RS cases (9 CLL-RS pairs, plus 3 paired terminal leukemic phases of RS). Diagnosis of CLL was based on IWCLL-NCI Working Group criteria (Hallek et al., 2008) and confirmed by a flow cytometry score >3, whereas diagnosis of RS was based on the histology of lymph node or extranodal tissue excisional biopsies. After institutional pathological review, all RS cases were classified as DLBCL according to the World Health Organization Classification of Tumors of the Hematopoietic and Lymphoid Tissues (Swerdlow, 2008). The clinical and biological features of the discovery cases are summarized in Table S1.

The screening panel used for additional CN analysis was composed of a multi-institutional cohort of 42 clonally related RS, 17 of which were also characterized by WES. An additional RS case with no CN data available was included in the WES-sequencing panel.

The cases included in this study were provided by the Division of Hematology, Department of Translational Medicine, Amedeo Avogadro University of Eastern Piedmont, Novara, Italy and by the Oncology Institute of Southern Switzerland (IOSI), Bellinzona, Switzerland. The study was approved by the Institutional Review Board of Columbia University and IOSI and by the Ethical Committee of the Azienda Ospedaliera Maggiore della Carità di Novara, Amedeo Avogadro University of Eastern Piedmont.

DNA extraction. High molecular-weight genomic DNA was extracted from samples according to standard procedures, quantitated by the Quant-iT Pico-Green reagent (Invitrogen) and verified for integrity by gel electrophoresis. Clonality of tumor samples was established by amplification of the rearranged Ig genes. The percentage of tumor cells of CLL and RSII samples was estimated by cytofluorometry analysis of CD5$^+$/CD19$^+$ cells in the peripheral blood, and the one of RS specimens by immunohistochemistry analysis of CD20$^+$/CD79a$^+$ cells in the correspondent RS section. In all phases, the percentage of tumor cells was then corrected based on the inferred CN value observed at the clonally rearranged Ig loci (i.e., the segment of intrachromosomal deletional recombination observed at the 14q32.33, 2p11.2, and 22q11.2 loci; Bergsagel and Kuehl, 2013). All analyzed cases had at least 35% of tumor cell content in the specimen used for WES and CN analyses (Table S1).

FISH and *IGHV* mutation analysis. The molecular characterization of RS cases, including FISH analysis and assessment of *IGHV* mutational status, was performed as previously described (Fabbri et al., 2011; Rossi et al., 2011b). In particular, the following probes were used for FISH analysis of the CLL-RS discovery pairs: (1) LSI13, LSID13S319, CEP12, LSIp53, LSIATM, LSI IGH/BCL2, LSI BCL6, LSI IGH/c-MYC/CEP8, c-MYC

break-apart, LSI N-MYC (Abbott); (2) *BCL3* split signal (Dako); (3) 6q21/α-satellite (Kreatech Biotechnology); and (4) bacterial artificial chromosome clones 373L24-rel and 440P05-BCL11A.

Whole-exome capture and massively parallel sequencing, sequence mapping, and identification of tumor-specific variants. Purified high molecular weight genomic DNA (∼1.5 µg) was enriched in protein-coding sequences using the SureSelect 50 Mb All Exon kit for the discovery cases and the SureSelect Human All Exon v4–51Mb for the screening cases (Agilent Technologies), following standard protocols. The resulting target-enriched pool was amplified and subjected to paired-end sequencing (2 × 100 bp) on the HiSeq2000 System. Exome capture and sequencing procedures were performed at St. Jude Children's Research Hospital, Fasteris, and Centrillion Biosciences. The mean depth of coverage for aligned reads was 83X (range, 34-158X), with ∼75% of the target sequence being covered by at least 30 reads (range, 48–89%). Based on a comparison with the heterozygous SNP call rate obtained in the same cases by analysis of Affymetrix SNP 6.0 array data (available for 20/21 samples), the sensitivity for the identification of heterozygous somatic mutations was estimated to be ∼97% (range, 94–99%). After filtering for duplicate reads (defined as reads with identical start and orientation), sequencing reads were mapped to the reference genome hg19 assembly (GRCh37) using the Burrows-Wheeler Aligner (BWA) alignment tool version 0.5.9 (Li and Durbin, 2010). Sequence variants (i.e., nucleotide substitutions and small insertions/deletions) were obtained using the SAVI (Statistical Algorithm for Variant Identification) algorithm independently for each sample (Tiacci et al., 2011). In brief, we constructed empirical priors for the distribution of variant frequencies in each sample independently and obtained high-credibility intervals (posterior probability ≥1−10^{-5}) for corresponding changes in frequency between any of the analyzed samples. Variants were considered absent when observed with a frequency between 0 and 2%, and present when showing a frequency ≥3%. Given a mean depth of coverage for aligned reads >80X across samples, we chose 3% as the lower threshold for detecting variants, considering a 1% error rate for the technology and a binomial distribution for the errors. Candidate variants were then filtered for (a) systematic errors known to be associated with the Illumina sequencing technology, (b) variants observed in only one strand, and (c) variants mapping to multiple loci in the genome, which may reflect captured pseudogenes and regions of low complexity. To this end, each variant with a flanking 35-base context sequence around its genomic position was mapped to the hg19 reference using the BLAST algorithm, and only variant reads with "unique mappability" were retained, that is, we required the 71-base sequence to uniquely map to the reference genome with only one mismatch. Candidate tumor-specific nonsilent variants were then obtained by subtracting (a) known polymorphisms reported in the NCBI dbSNP database (Build 137); (b) variants present in any one of 105 exomes from unaffected individuals analyzed at our institution; and (c) silent mutations. In addition, splice site variants were kept only if located within 4 nt of a consensus splice site.

As the percentage of tumoral cells present in the analyzed specimens was not homogeneous across samples (Table S1), we corrected the variants' frequencies by calculating the expected frequency based on the total depth of the variant, its observed frequency, and the tumor content of the sample, assuming a binomial distribution. Mutations were classified as clonal if the fraction of variant reads was >20 (upon correction for the percentage of tumor cells in the sample), and subclonal otherwise.

The genomic positions of the candidate variants were converted to the hg18 coordinates using the LiftOver tool (UCSC Genome Browser) to be consistent with the annotation used to report CN aberrations.

For the purpose of deciphering the history of clonal evolution during CLL transformation to RS, CLL-only variants were defined as events clonally represented in CLL and absent or subclonal in RS and/or RSII and RS-only variants included events clonally represented in RS and absent/subclonal in CLL or subclonal in RS and absent in CLL. The same criteria were applied to identify RSII-only variants. To establish whether the difference in representation of the variants in distinct disease phases was statistically significant, we calculated the probability of observing the variant's depth, given its position

total depth, its observed frequency in the paired sample, and the estimates for samples' tumor contents, using a binomial distribution. Variants with p-values >0.05 were discarded.

Previously reported genetic lesions detected in the same cases by Sanger sequencing (*TP53*, *NOTCH1*, and *SF3B1*) were all correctly identified by our approach (Table S1). Only one 50-bp duplication affecting the PEST domain of *NOTCH1* was missed by WES, consistent with the lower sensitivity of our mutation discovery algorithm in detecting large insertions and deletions. A set of candidate RS-specific nonsilent somatic mutations were subjected to validation by conventional Sanger-based resequencing analysis of PCR products obtained from tumor DNA using primers specific for the exon encompassing the variant, as previously described (Fabbri et al., 2011; Pasqualucci et al., 2011). The validation rate of a subset of the identified point mutations tested by Sanger sequencing was ∼94% ($n = 133/141$).

Given the absence of paired normal DNAs, SAVI was used to interrogate a specific list of target genes ($n = 481$) in the WES-screening panel, as described in the section "Recurrent targets of point mutations in RS."

CN analysis by high–density SNP array analysis. Genome-wide DNA profiles from 50 RS samples, of which 14 with paired CLL, including 8 out of 9 discovery RS cases, 3 RS-leukemic phases, and a series of normal samples ($n = 7$) were obtained from high molecular weight genomic DNA using the Affymetrix Genome-Wide Human SNP Array 6.0 (Affymetrix) and standard protocols from Affymetrix as previously described (Fabbri et al., 2011; Pasqualucci et al., 2011). Previously reported genetic lesions detected by FISH–based analysis (when present in >25% of nuclei) were all correctly identified by our approach (Table S1). Data analysis, including the identification of Minimal Common Regions of aberration and the Genomic Identification of Significant Targets in Cancer (GISTIC), was performed as previously described (Fabbri et al., 2011; Pasqualucci et al., 2011). In brief, we focused on focal MCRs encompassing ≤3 protein-coding genes and not determined by the overlap between large segments (i.e., >1 Mb; Pasqualucci et al., 2011). Recurrent focal MCRs are shown in Fig. 4 b and significant regions of loss and gain as assessed by GISTIC are reported in Fig. 4 d.

Identification of significant association and mutual exclusion between RS-associated genetic lesions. To determine the independence of any two genetic events occurring in the RS cases, we counted the number of samples involved in both events and calculated a p-value according to the hypergeometric distribution. If the number was significantly larger than expected, the two events were considered comutated, whereas if the number was significantly smaller they were considered mutually exclusive. We used a p-value threshold of 0.05 to assess the significance of both mutual-exclusion and comutation. Due to the limited number of samples, we did not use multi-test correlation in this experiment.

Functional categories and pathways analyses of the mutated genes. Genes found to be altered in RS were assigned to functional categories or to annotated pathways using the gene ontology GO database (http://www.geneontology.org/), the publicly available bioinformatic tool DAVID 2008 6.7 (Database for Annotation, Visualization and Integrated Discovery, http://david.abcc.ncifcrf.gov/), and the Molecular Signatures Database from the Broad Institute (MSigDBv4.0, http://www.broadinstitute.org/gsea/msigdb/index.jsp). In brief, the functional annotation chart tool of DAVID 2008 was used to identify enriched functional categories associated with RS-altered genes (including the "GOTERM_BP_ALL" and the "Pathways" terms); the Compute Overlap tool of the Molecular Signatures Database was used to examine how the gene set composed by RS-altered genes overlapped with gene sets belonging to the C2-Canonical pathways collection. DAVID 2008 categories and MSigDB overlaps were then selected to retain only those with a P value ≤0.05.

Accession nos. Affymetrix SNP Array 6.0 data and WES data have been deposited in dbGaP under accession no. phs000364.v2.p1.

Online supplemental material. Table S1 shows clinical and biological features of the 9 CLL-RS discovery cases; Table S2 reports mutations identified by WES in the discovery and screening panels; and Table S3 illustrates the segments (regions) of tumor-acquired CN alterations identified in the discovery panel and in additional six paired and clonally related CLL-RS pairs. Online supplemental material is available at http://www.jem.org/cgi/content/full/jem.20131448/DC1.

REFERENCES

Annunziata, C.M., R.E. Davis, Y. Demchenko, W. Bellamy, A. Gabrea, F. Zhan, G. Lenz, I. Hanamura, G. Wright, W. Xiao, et al. 2007. Frequent engagement of the classical and alternative NF-kappaB pathways by diverse genetic abnormalities in multiple myeloma. *Cancer Cell.* 12:115–130. http://dx.doi.org/10.1016/j.ccr.2007.07.004

Aparicio, S., and C. Caldas. 2013. The implications of clonal genome evolution for cancer medicine. *N. Engl. J. Med.* 368:842–851. http://dx.doi.org/10.1056/NEJMra1204892

Baumann, P., and T.R. Cech. 2001. Pot1, the putative telomere end-binding protein in fission yeast and humans. *Science.* 292:1171–1175. http://dx.doi.org/10.1126/science.1060036

Berger, M.F., E. Hodis, T.P. Heffernan, Y.L. Deribe, M.S. Lawrence, A. Protopopov, E. Ivanova, I.R. Watson, E. Nickerson, P. Ghosh, et al. 2012. Melanoma genome sequencing reveals frequent PREX2 mutations. *Nature.* 485:502–506.

Bergsagel, P.L., and W.M. Kuehl. 2013. Degree of focal immunoglobulin heavy chain locus deletion as a measure of B-cell tumor purity. *Leukemia.* (Epub ahead of print).

Berlin, I., H. Schwartz, and P.D. Nash. 2010. Regulation of epidermal growth factor receptor ubiquitination and trafficking by the USP8·STAM complex. *J. Biol. Chem.* 285:34909–34921. http://dx.doi.org/10.1074/jbc.M109.016287

Beroukhim, R., G. Getz, L. Nghiemphu, J. Barretina, T. Hsueh, D. Linhart, I. Vivanco, J.C. Lee, J.H. Huang, S. Alexander, et al. 2007. Assessing the significance of chromosomal aberrations in cancer: methodology and application to glioma. *Proc. Natl. Acad. Sci. USA.* 104:20007–20012. http://dx.doi.org/10.1073/pnas.0710052104

Bories, J.C., D.M. Willerford, D. Grévin, L. Davidson, A. Camus, P. Martin, D. Stéhelin, and F.W. Alt. 1995. Increased T-cell apoptosis and terminal B-cell differentiation induced by inactivation of the Ets-1 proto-oncogene. *Nature.* 377:635–638. http://dx.doi.org/10.1038/377635a0

Carlotti, E., D. Wrench, J. Matthews, S. Iqbal, A. Davies, A. Norton, J. Hart, R. Lai, S. Montoto, J.G. Gribben, et al. 2009. Transformation of follicular lymphoma to diffuse large B-cell lymphoma may occur by divergent evolution from a common progenitor cell or by direct evolution from the follicular lymphoma clone. *Blood*. 113:3553–3557. http://dx.doi.org/10.1182/blood-2008-08-174839

Challa-Malladi, M., Y.K. Lieu, O. Califano, A.B. Holmes, G. Bhagat, V.V. Murty, D. Dominguez-Sola, L. Pasqualucci, and R. Dalla-Favera. 2011. Combined genetic inactivation of β2-Microglobulin and CD58 reveals frequent escape from immune recognition in diffuse large B cell lymphoma. *Cancer Cell*. 20:728–740. http://dx.doi.org/10.1016/j.ccr.2011.11.006

Coiffier, B., E. Lepage, J. Briere, R. Herbrecht, H. Tilly, R. Bouabdallah, P. Morel, E. Van Den Neste, G. Salles, P. Gaulard, et al. 2002. CHOP chemotherapy plus rituximab compared with CHOP alone in elderly patients with diffuse large-B-cell lymphoma. *N. Engl. J. Med.* 346:235–242. http://dx.doi.org/10.1056/NEJMoa011795

Davies, A.J., A. Rosenwald, G. Wright, A. Lee, K.W. Last, D.D. Weisenburger, W.C. Chan, J. Delabie, R.M. Braziel, E. Campo, et al. 2007. Transformation of follicular lymphoma to diffuse large B-cell lymphoma proceeds by distinct oncogenic mechanisms. *Br. J. Haematol.* 136:286–293. http://dx.doi.org/10.1111/j.1365-2141.2006.06439.x

Domen, J., N.M. van der Lugt, D. Acton, P.W. Laird, K. Linders, and A. Berns. 1993. Pim-1 levels determine the size of early B lymphoid compartments in bone marrow. *J. Exp. Med.* 178:1665–1673. http://dx.doi.org/10.1084/jem.178.5.1665

Edelmann, J., K. Holzmann, F. Miller, D. Winkler, A. Bühler, T. Zenz, L. Bullinger, M.W. Kühn, A. Gerhardinger, J. Bloehdorn, et al. 2012. High-resolution genomic profiling of chronic lymphocytic leukemia reveals new recurrent genomic alterations. *Blood*. 120:4783–4794. http://dx.doi.org/10.1182/blood-2012-04-423517

Fabbri, G., S. Rasi, D. Rossi, V. Trifonov, H. Khiabanian, J. Ma, A. Grunn, M. Fangazio, D. Capello, S. Monti, et al. 2011. Analysis of the chronic lymphocytic leukemia coding genome: role of NOTCH1 mutational activation. *J. Exp. Med.* 208:1389–1401. http://dx.doi.org/10.1084/jem.20110921

Fine, B., C. Hodakoski, S. Koujak, T. Su, L.H. Saal, M. Maurer, B. Hopkins, M. Keniry, M.L. Sulis, S. Mense, et al. 2009. Activation of the PI3K pathway in cancer through inhibition of PTEN by exchange factor P-REX2a. *Science*. 325:1261–1265. http://dx.doi.org/10.1126/science.1173569

Golas, M.M., B. Sander, C.L. Will, R. Lührmann, and H. Stark. 2003. Molecular architecture of the multiprotein splicing factor SF3b. *Science*. 300:980–984. http://dx.doi.org/10.1126/science.1084155

Grasso, C.S., Y.M. Wu, D.R. Robinson, X. Cao, S.M. Dhanasekaran, A.P. Khan, M.J. Quist, X. Jing, R.J. Lonigro, J.C. Brenner, et al. 2012. The mutational landscape of lethal castration-resistant prostate cancer. *Nature*. 487:239–243. http://dx.doi.org/10.1038/nature11125

Hallek, M., B.D. Cheson, D. Catovsky, F. Caligaris-Cappio, G. Dighiero, H. Döhner, P. Hillmen, M.J. Keating, E. Montserrat, K.R. Rai, and T.J. Kipps; International Workshop on Chronic Lymphocytic Leukemia. 2008. Guidelines for the diagnosis and treatment of chronic lymphocytic leukemia: a report from the International Workshop on Chronic Lymphocytic Leukemia updating the National Cancer Institute-Working Group 1996 guidelines. *Blood*. 111:5446–5456. http://dx.doi.org/10.1182/blood-2007-06-093906

Hannon, G.J., and D. Beach. 1994. p15INK4B is a potential effector of TGF-beta-induced cell cycle arrest. *Nature*. 371:257–261. http://dx.doi.org/10.1038/371257a0

Hans, C.P., D.D. Weisenburger, T.C. Greiner, R.D. Gascoyne, J. Delabie, G. Ott, H.K. Müller-Hermelink, E. Campo, R.M. Braziel, E.S. Jaffe, et al. 2004. Confirmation of the molecular classification of diffuse large B-cell lymphoma by immunohistochemistry using a tissue microarray. *Blood*. 103:275–282. http://dx.doi.org/10.1182/blood-2003-05-1545

He, L., J.M. Thomson, M.T. Hemann, E. Hernando-Monge, D. Mu, S. Goodson, S. Powers, C. Cordon-Cardo, S.W. Lowe, G.J. Hannon, and S.M. Hammond. 2005. A microRNA polycistron as a potential human oncogene. *Nature*. 435:828–833. http://dx.doi.org/10.1038/nature03552

Huang, W., B.T. Sherman, and R.A. Lempicki. 2009a. Bioinformatics enrichment tools: paths toward the comprehensive functional analysis of large gene lists. *Nucleic Acids Res.* 37:1–13. http://dx.doi.org/10.1093/nar/gkn923

Huang, W., B.T. Sherman, and R.A. Lempicki. 2009b. Systematic and integrative analysis of large gene lists using DAVID bioinformatics resources. *Nat. Protoc.* 4:44–57. http://dx.doi.org/10.1038/nprot.2008.211

Huang, F.W., E. Hodis, M.J. Xu, G.V. Kryukov, L. Chin, and L.A. Garraway. 2013. Highly recurrent TERT promoter mutations in human melanoma. *Science*. 339:957–959. http://dx.doi.org/10.1126/science.1229259

Keats, J.J., R. Fonseca, M. Chesi, R. Schop, A. Baker, W.J. Chng, S. Van Wier, R. Tiedemann, C.X. Shi, M. Sebag, et al. 2007. Promiscuous mutations activate the noncanonical NF-kappaB pathway in multiple myeloma. *Cancer Cell*. 12:131–144. http://dx.doi.org/10.1016/j.ccr.2007.07.003

Kikushige, Y., F. Ishikawa, T. Miyamoto, T. Shima, S. Urata, G. Yoshimoto, Y. Mori, T. Iino, T. Yamauchi, T. Eto, et al. 2011. Self-renewing hematopoietic stem cell is the primary target in pathogenesis of human chronic lymphocytic leukemia. *Cancer Cell*. 20:246–259. http://dx.doi.org/10.1016/j.ccr.2011.06.029

Kulis, M., S. Heath, M. Bibikova, A.C. Queirós, A. Navarro, G. Clot, A. Martínez-Trillos, G. Castellano, I. Brun-Heath, M. Pinyol, et al. 2012. Epigenomic analysis detects widespread gene-body DNA hypomethylation in chronic lymphocytic leukemia. *Nat. Genet.* 44:1236–1242. http://dx.doi.org/10.1038/ng.2443

Küppers, R., and R. Dalla-Favera. 2001. Mechanisms of chromosomal translocations in B cell lymphomas. *Oncogene*. 20:5580–5594. http://dx.doi.org/10.1038/sj.onc.1204640

Kuroda, K., H. Han, S. Tani, K. Tanigaki, T. Tun, T. Furukawa, Y. Taniguchi, H. Kurooka, Y. Hamada, S. Toyokuni, and T. Honjo. 2003. Regulation of marginal zone B cell development by MINT, a suppressor of Notch/RBP-J signaling pathway. *Immunity*. 18:301–312. http://dx.doi.org/10.1016/S1074-7613(03)00029-3

Landau, D.A., S.L. Carter, P. Stojanov, A. McKenna, K. Stevenson, M.S. Lawrence, C. Sougnez, C. Stewart, A. Sivachenko, L. Wang, et al. 2013. Evolution and impact of subclonal mutations in chronic lymphocytic leukemia. *Cell*. 152:714–726. http://dx.doi.org/10.1016/j.cell.2013.01.019

Li, H., and R. Durbin. 2010. Fast and accurate long-read alignment with Burrows-Wheeler transform. *Bioinformatics*. 26:589–595. http://dx.doi.org/10.1093/bioinformatics/btp698

Lohr, J.G., P. Stojanov, M.S. Lawrence, D. Auclair, B. Chapuy, C. Sougnez, P. Cruz-Gordillo, B. Knoechel, Y.W. Asmann, S.L. Slager, et al. 2012. Discovery and prioritization of somatic mutations in diffuse large B-cell lymphoma (DLBCL) by whole-exome sequencing. *Proc. Natl. Acad. Sci. USA*. 109:3879–3884. http://dx.doi.org/10.1073/pnas.1121343109

Lui, T.T., C. Lacroix, S.M. Ahmed, S.J. Goldenberg, C.A. Leach, A.M. Daulat, and S. Angers. 2011. The ubiquitin-specific protease USP34 regulates axin stability and Wnt/β-catenin signaling. *Mol. Cell. Biol.* 31:2053–2065. http://dx.doi.org/10.1128/MCB.01094-10

Monti, S., B. Chapuy, K. Takeyama, S.J. Rodig, Y. Hao, K.T. Yeda, H. Inguilizian, C. Mermel, T. Currie, A. Dogan, et al. 2012. Integrative analysis reveals an outcome-associated and targetable pattern of p53 and cell cycle deregulation in diffuse large B cell lymphoma. *Cancer Cell*. 22:359–372. http://dx.doi.org/10.1016/j.ccr.2012.07.014

Mootha, V.K., C.M. Lindgren, K.F. Eriksson, A. Subramanian, S. Sihag, J. Lehar, P. Puigserver, E. Carlsson, M. Ridderstråle, E. Laurila, et al. 2003. PGC-1alpha-responsive genes involved in oxidative phosphorylation are coordinately downregulated in human diabetes. *Nat. Genet.* 34:267–273. http://dx.doi.org/10.1038/ng1180

Morin, R.D., M. Mendez-Lago, A.J. Mungall, R. Goya, K.L. Mungall, R.D. Corbett, N.A. Johnson, T.M. Severson, R. Chiu, M. Field, et al. 2011. Frequent mutation of histone-modifying genes in non-Hodgkin lymphoma. *Nature*. 476:298–303. http://dx.doi.org/10.1038/nature10351

Ouillette, P., S. Fossum, B. Parkin, L. Ding, P. Bockenstedt, A. Al-Zoubi, K. Shedden, and S.N. Malek. 2010. Aggressive chronic lymphocytic leukemia with elevated genomic complexity is associated with multiple gene defects in the response to DNA double-strand breaks. *Clin. Cancer Res.* 16:835–847. http://dx.doi.org/10.1158/1078-0432.CCR-09-2534

Ouillette, P., K. Saiya-Cork, E. Seymour, C. Li, K. Shedden, and S.N. Malek. 2013. Clonal evolution, genomic drivers, and effects of therapy

in chronic lymphocytic leukemia. *Clin. Cancer Res.* 19:2893–2904. http://dx.doi.org/10.1158/1078-0432.CCR-13-0138

Palomero, T., W.K. Lim, D.T. Odom, M.L. Sulis, P.J. Real, A. Margolin, K.C. Barnes, J. O'Neil, D. Neuberg, A.P. Weng, et al. 2006. NOTCH1 directly regulates c-MYC and activates a feed-forward-loop transcriptional network promoting leukemic cell growth. *Proc. Natl. Acad. Sci. USA.* 103:18261–18266. http://dx.doi.org/10.1073/pnas.0606108103

Pasqualucci, L., V. Trifonov, G. Fabbri, J. Ma, D. Rossi, A. Chiarenza, V.A. Wells, A. Grunn, M. Messina, O. Elliot, et al. 2011. Analysis of the coding genome of diffuse large B-cell lymphoma. *Nat. Genet.* 43:830–837. http://dx.doi.org/10.1038/ng.892

Puente, X.S., M. Pinyol, V. Quesada, L. Conde, G.R. Ordóñez, N. Villamor, G. Escaramis, P. Jares, S. Beà, M. González-Díaz, et al. 2011. Whole-genome sequencing identifies recurrent mutations in chronic lymphocytic leukaemia. *Nature.* 475:101–105. http://dx.doi.org/10.1038/nature10113

Quesada, V., L. Conde, N. Villamor, G.R. Ordóñez, P. Jares, L. Bassaganyas, A.J. Ramsay, S. Beà, M. Pinyol, A. Martínez-Trillos, et al. 2012. Exome sequencing identifies recurrent mutations of the splicing factor SF3B1 gene in chronic lymphocytic leukemia. *Nat. Genet.* 44:47–52. http://dx.doi.org/10.1038/ng.1032

Ramsay, A.J., V. Quesada, M. Foronda, L. Conde, A. Martínez-Trillos, N. Villamor, D. Rodríguez, A. Kwarciak, C. Garabaya, M. Gallardo, et al. 2013. POT1 mutations cause telomere dysfunction in chronic lymphocytic leukemia. *Nat. Genet.* 45:526–530. http://dx.doi.org/10.1038/ng.2584

Rausch, T., D.T. Jones, M. Zapatka, A.M. Stütz, T. Zichner, J. Weischenfeldt, N. Jäger, M. Remke, D. Shih, P.A. Northcott, et al. 2012. Genome sequencing of pediatric medulloblastoma links catastrophic DNA rearrangements with TP53 mutations. *Cell.* 148:59–71. http://dx.doi.org/10.1016/j.cell.2011.12.013

Rawlings, D.J., M.A. Schwartz, S.W. Jackson, and A. Meyer-Bahlburg. 2012. Integration of B cell responses through Toll-like receptors and antigen receptors. *Nat. Rev. Immunol.* 12:282–294. http://dx.doi.org/10.1038/nri3190

Rossi, D., and G. Gaidano. 2009. Richter syndrome: molecular insights and clinical perspectives. *Hematol. Oncol.* 27:1–10. http://dx.doi.org/10.1002/hon.880

Rossi, D., M. Cerri, D. Capello, C. Deambrogi, F.M. Rossi, A. Zucchetto, L. De Paoli, S. Cresta, S. Rasi, V. Spina, et al. 2008. Biological and clinical risk factors of chronic lymphocytic leukaemia transformation to Richter syndrome. *Br. J. Haematol.* 142:202–215. http://dx.doi.org/10.1111/j.1365-2141.2008.07166.x

Rossi, D., A. Bruscaggin, V. Spina, S. Rasi, H. Khiabanian, M. Messina, M. Fangazio, T. Vaisitti, S. Monti, S. Chiaretti, et al. 2011a. Mutations of the SF3B1 splicing factor in chronic lymphocytic leukemia: association with progression and fludarabine-refractoriness. *Blood.* 118:6904–6908. http://dx.doi.org/10.1182/blood-2011-08-373159

Rossi, D., V. Spina, C. Deambrogi, S. Rasi, L. Laurenti, K. Stamatopoulos, L. Arcaini, M. Lucioni, G.B. Rocque, Z.Y. Xu-Monette, et al. 2011b. The genetics of Richter syndrome reveals disease heterogeneity and predicts survival after transformation. *Blood.* 117:3391–3401. http://dx.doi.org/10.1182/blood-2010-09-302174

Rossi, D., M. Fangazio, S. Rasi, T. Vaisitti, S. Monti, S. Cresta, S. Chiaretti, I. Del Giudice, G. Fabbri, A. Bruscaggin, et al. 2012a. Disruption of BIRC3 associates with fludarabine chemorefractoriness in TP53 wild-type chronic lymphocytic leukemia. *Blood.* 119:2854–2862. http://dx.doi.org/10.1182/blood-2011-12-395673

Rossi, D., V. Spina, F. Forconi, D. Capello, M. Fangazio, S. Rasi, M. Martini, V. Gattei, A. Ramponi, L.M. Larocca, et al. 2012b. Molecular history of Richter syndrome: origin from a cell already present at the time of chronic lymphocytic leukemia diagnosis. *Int. J. Cancer.* 130:3006–3010. http://dx.doi.org/10.1002/ijc.26322

Rossi, D., V. Trifonov, M. Fangazio, A. Bruscaggin, S. Rasi, V. Spina, S. Monti, T. Vaisitti, F. Arruga, R. Famà, et al. 2012c. The coding genome of splenic marginal zone lymphoma: activation of NOTCH2 and other pathways regulating marginal zone development. *J. Exp. Med.* 209:1537–1551. http://dx.doi.org/10.1084/jem.20120904

Saito, T., S. Chiba, M. Ichikawa, A. Kunisato, T. Asai, K. Shimizu, T. Yamaguchi, G. Yamamoto, S. Seo, K. Kumano, et al. 2003. Notch2

is preferentially expressed in mature B cells and indispensable for marginal zone B lineage development. *Immunity.* 18:675–685. http://dx.doi.org/10.1016/S1074-7613(03)00111-0

Samon, J.B., M. Castillo-Martin, M. Hadler, A. Ambesi-Impiobato, E. Paietta, J. Racevskis, P.H. Wiernik, J.M. Rowe, J. Jakubczak, S. Randolph, et al. 2012. Preclinical analysis of the γ-secretase inhibitor PF-03084014 in combination with glucocorticoids in T-cell acute lymphoblastic leukemia. *Mol. Cancer Ther.* 11:1565–1575. http://dx.doi.org/10.1158/1535-7163.MCT-11-0938

Schuh, A., J. Becq, S. Humphray, A. Alexa, A. Burns, R. Clifford, S.M. Feller, R. Grocock, S. Henderson, I. Khrebtukova, et al. 2012. Monitoring chronic lymphocytic leukemia progression by whole genome sequencing reveals heterogeneous clonal evolution patterns. *Blood.* 120:4191–4196. http://dx.doi.org/10.1182/blood-2012-05-433540

Serrano, M., G.J. Hannon, and D. Beach. 1993. A new regulatory motif in cell-cycle control causing specific inhibition of cyclin D/CDK4. *Nature.* 366:704–707. http://dx.doi.org/10.1038/366704a0

Sherr, C.J. 2004. Principles of tumor suppression. *Cell.* 116:235–246. http://dx.doi.org/10.1016/S0092-8674(03)01075-4

Stankovic, T., P. Weber, G. Stewart, T. Bedenham, J. Murray, P.J. Byrd, P.A. Moss, and A.M. Taylor. 1999. Inactivation of ataxia telangiectasia mutated gene in B-cell chronic lymphocytic leukaemia. *Lancet.* 353:26–29. http://dx.doi.org/10.1016/S0140-6736(98)10117-4

Subramanian, A., P. Tamayo, V.K. Mootha, S. Mukherjee, B.L. Ebert, M.A. Gillette, A. Paulovich, S.L. Pomeroy, T.R. Golub, E.S. Lander, and J.P. Mesirov. 2005. Gene set enrichment analysis: a knowledge-based approach for interpreting genome-wide expression profiles. *Proc. Natl. Acad. Sci. USA.* 102:15545–15550. http://dx.doi.org/10.1073/pnas.0506580102

Sun, X., H.F. Frierson, C. Chen, C. Li, Q. Ran, K.B. Otto, B.L. Cantarel, R.L. Vessella, A.C. Gao, J. Petros, et al. 2005. Frequent somatic mutations of the transcription factor ATBF1 in human prostate cancer. *Nat. Genet.* 37:407–412. http://dx.doi.org/10.1038/ng1528

Swerdlow, S.H. 2008. WHO Classification of Tumours of Haematopoetic and Lymphoid Tissues. *International Agency for research on Cancer (IARC), Lyon*

Tiacci, E., V. Trifonov, G. Schiavoni, A. Holmes, W. Kern, M.P. Martelli, A. Pucciarini, B. Bigerna, R. Pacini, V.A. Wells, et al. 2011. BRAF mutations in hairy-cell leukemia. *N. Engl. J. Med.* 364:2305–2315. http://dx.doi.org/10.1056/NEJMoa1014209

Tsimberidou, A.M., S. O'Brien, I. Khouri, F.J. Giles, H.M. Kantarjian, R. Champlin, S. Wen, K.A. Do, S.C. Smith, S. Lerner, et al. 2006. Clinical outcomes and prognostic factors in patients with Richter's syndrome treated with chemotherapy or chemoimmunotherapy with or without stem-cell transplantation. *J. Clin. Oncol.* 24:2343–2351. http://dx.doi.org/10.1200/JCO.2005.05.0187

Tsimberidou, A.M., W.G. Wierda, W. Plunkett, R. Kurzrock, S. O'Brien, S. Wen, A. Ferrajoli, F. Ravandi-Kashani, G. Garcia-Manero, Z. Estrov, et al. 2008. Phase I-II study of oxaliplatin, fludarabine, cytarabine, and rituximab combination therapy in patients with Richter's syndrome or fludarabine-refractory chronic lymphocytic leukemia. *J. Clin. Oncol.* 26:196–203. http://dx.doi.org/10.1200/JCO.2007.11.8513

Vaux, D.L., S. Cory, and J.M. Adams. 1988. Bcl-2 gene promotes haemopoietic cell survival and cooperates with c-myc to immortalize pre-B cells. *Nature.* 335:440–442. http://dx.doi.org/10.1038/335440a0

Walter, M.J., D. Shen, L. Ding, J. Shao, D.C. Koboldt, K. Chen, D.E. Larson, M.D. McLellan, D. Dooling, R. Abbott, et al. 2012. Clonal architecture of secondary acute myeloid leukemia. *N. Engl. J. Med.* 366:1090–1098. http://dx.doi.org/10.1056/NEJMoa1106968

Wang, H., and H.C. Morse III. 2009. IRF8 regulates myeloid and B lymphoid lineage diversification. *Immunol. Res.* 43:109–117. http://dx.doi.org/10.1007/s12026-008-8055-8

Wang, L., M.S. Lawrence, Y. Wan, P. Stojanov, C. Sougnez, K. Stevenson, L. Werner, A. Sivachenko, D.S. DeLuca, L. Zhang, et al. 2011. SF3B1 and other novel cancer genes in chronic lymphocytic leukemia. *N. Engl. J. Med.* 365:2497–2506. http://dx.doi.org/10.1056/NEJMoa1109016

Weng, A.P., A.A. Ferrando, W. Lee, J.P. Morris IV, L.B. Silverman, C. Sanchez-Irizarry, S.C. Blacklow, A.T. Look, and J.C. Aster. 2004.

Activating mutations of NOTCH1 in human T cell acute lymphoblastic leukemia. *Science*. 306:269–271. http://dx.doi.org/10.1126/science .1102160

Wu, J.N., and C.W. Roberts. 2013. ARID1A Mutations in Cancer: Another Epigenetic Tumor Suppressor? *Cancer discovery*. 3:35-43.

Wu, Y., C. Cain-Hom, L. Choy, T.J. Hagenbeek, G.P. de Leon, Y. Chen, D. Finkle, R.Venook, X.Wu, J. Ridgway, et al. 2010.Therapeutic antibody targeting of individual Notch receptors. *Nature*. 464:1052–1057. http://dx.doi.org/10.1038/nature08878

Xiao, C., L. Srinivasan, D.P. Calado, H.C. Patterson, B. Zhang, J. Wang, J.M. Henderson, J.L. Kutok, and K. Rajewsky. 2008. Lymphoproliferative disease and autoimmunity in mice with increased miR-17-92 expression in lymphocytes. *Nat. Immunol.* 9:405–414. http://dx.doi.org/10 .1038/ni1575

Yano, T., E.S. Jaffe, D.L. Longo, and M. Raffeld. 1992. MYC rearrangements in histologically progressed follicular lymphomas. *Blood*. 80:758–767.

Zenz, T., B. Eichhorst, R. Busch, T. Denzel, S. Häbe, D. Winkler, A. Bühler, J. Edelmann, M. Bergmann, G. Hopfinger, et al. 2010. TP53 mutation and survival in chronic lymphocytic leukemia. *J. Clin. Oncol.* 28:4473–4479. http://dx.doi.org/10.1200/JCO.2009.27.8762

Zhang, Y., Y. Xiong, and W.G. Yarbrough. 1998. ARF promotes MDM2 degradation and stabilizes p53: ARF-INK4a locus deletion impairs both the Rb and p53 tumor suppression pathways. *Cell*. 92:725–734. http:// dx.doi.org/10.1016/S0092-8674(00)81401-4

Zhang, J., V. Grubor, C.L. Love, A. Banerjee, K.L. Richards, P.A. Mieczkowski, C. Dunphy, W. Choi, W.Y. Au, G. Srivastava, et al. 2013. Genetic heterogeneity of diffuse large B-cell lymphoma. *Proceedings of the National Academy of Sciences of the United States of America*.